⌘ *Author's Choice*

THE JOURNAL OF BIOLOGICAL CHEMISTRY VOL. 285, NO. 23, pp. 17628–17635, June 4, 2010
© 2010 by The American Society for Biochemistry and Molecular Biology, Inc. Printed in the U.S.A.

Novel Binding of the Mitotic Regulator TPX2 (Target Protein for *Xenopus* Kinesin-like Protein 2) to Importin-α*

Received for publication, January 8, 2010, and in revised form, March 10, 2010 Published, JBC Papers in Press, March 23, 2010, DOI 10.1074/jbc.M110.102343

Astrid Giesecke[1] **and Murray Stewart**[2]

From the Medical Research Council Laboratory of Molecular Biology, Cambridge CB2 0QH, United Kingdom

Several aspects of mitotic spindle assembly are orchestrated by the Ran GTPase through its modulation of the interaction between spindle assembly factors and importin-α. One such factor is TPX2 that promotes microtubule assembly in the vicinity of chromosomes. TPX2 is inhibited when bound to importin-α, which occurs when the latter is bound to importin-β. The importin-α:β interaction is disrupted by the high RanGTP concentration near the chromosomes, releasing TPX2. In more distal regions, where Ran is predominantly GDP-bound, TPX2 remains bound to importin-α and so is inhibited. Here we use a combination of structural and biochemical methods to define the basis for TPX2 binding to importin-α. A 2.2 Å resolution crystal structure shows that the primary nuclear localization signal (^{284}KRKH^{287}) of TPX2, which has been shown to be crucial for inhibition, binds to the minor NLS-binding site on importin-α. This atypical interaction pattern was confirmed using complementary binding studies that employed importin-α variants in which binding to either the major or minor NLS-binding site was impaired, together with competition assays using the SV40 monopartite NLS that binds primarily to the major site. The different way in which TPX2 binds to importin-α could account for much of the selectivity necessary during mitosis because this would reduce the competition for binding to importin-α from other NLS-containing proteins.

In many species, the generation of the mitotic spindle is orchestrated by the RanGTPase (1–4), which, during interphase, powers many nuclear trafficking pathways (5, 6). In both mitosis and nuclear trafficking, Ran functions by modulating the interaction between nuclear transport factors and a range of target proteins. Thus, in nuclear protein import, for example, cargo proteins destined for nuclear import bind to transport factors (importins) in the cytoplasm, where Ran is in the GDP-bound form. This cargo:carrier complex then equilibrates between the two compartments through nuclear pore complexes (NPCs). In the nucleus, RanGTP dissociates the import complex, releasing the cargo, after which the transport factors are recycled to the cytoplasm where the Ran GTP is hydrolyzed, freeing the transport factors for another import cycle. However, during an open mitosis, the nuclear envelope is disassembled and instead Ran and some nuclear transport factors are used to orchestrate microtubule dynamics related to spindle generation (reviewed in Ref. 3).

TPX2 (**t**arget **p**rotein for *Xenopus* kinesin-like protein **2**)[3] is a microtubule assembly factor involved in chromatin-promoted spindle assembly and this activity is orchestrated by Ran (1, 7–10). Ran is maintained in the GTP-bound form near the chromosomes, but is in the GDP-bound form in more distal regions (11). In the absence of RanGTP, the nuclear protein import factor importin-β binds to the importin-α adaptor, and this interaction frees importin-α to bind molecules such as TPX2 that have a nuclear localization sequence (NLS). A common form of NLS is the "classical" NLS that contain one ("monopartite") or two ("bipartite") clusters of basic residues (12). The microtubule assembly function of TPX2 is inhibited when it is sequestered by importin-α. However, in the vicinity of the chromosomes, RanGTP binds to importin-β, releasing importin-α. The importin-β binding domain of importin-α (the IBB domain) in combination with other factors (6, 12–15) then displaces NLS-containing cargoes such as TPX2, freeing them to participate in spindle assembly, as illustrated schematically in Fig. 1. It was originally proposed that TPX2 functioned in spindle assembly through an interaction between its N terminus and the Aurora A kinase (1). This interaction is important in regulating Aurora A activity and, for example, the reduced cellular activity and mislocalization the Aurora A(S155R) mutant protein are because of loss of interaction with TPX2 (16). However, subsequent studies have indicated that the C terminus of TPX2 is crucial for its microtubule nucleation function, possibly by way of interacting with the kinesin-like protein Xklp2 and targeting it to the spindle poles (17–19) and/or by influencing kinetochore-associated microtubule formation (10). Overall, TPX2 appears to represent a key node in a complex network of protein:protein interactions that is required for spindle assembly (10, 17).

Previous work on the binding of classical NLSs to importin-α has established consensus sequence motifs for both monopartite and bipartite NLSs and has examined the contributions made by the different side chains involved (reviewed in Ref. 12). Importin-α is a banana-shaped molecule constructed from a

* This work was supported in part by a Wellcome Trust Programme grant (to M. S.).

⌘ *Author's Choice*—Final version full access.

The atomic coordinates and structure factors (code 3KND) have been deposited in the Protein Data Bank, Research Collaboratory for Structural Bioinformatics, Rutgers University, New Brunswick, NJ (http://www.rcsb.org/).

[1] Present address: GlaxoSmithKline UK Ltd., Gunnels Wood Road, Stevenage SG1 2NY, UK.

[2] To whom correspondence should be addressed: MRC Laboratory of Molecular Biology, Hills Rd., Cambridge CB2 0QH, UK. Tel.: 44-1223-402463; Fax: 44-1223-213556; E-mail: ms@mrc-lmb.cam.ac.uk.

[3] The abbreviations used are: TPX2, target protein for *Xenopus* kinesin-like protein 2; NLS, nuclear localization sequence; IBB, importin-β binding; DTT, dithiothreitol; PDB, Protein Data Bank; GST, glutathione *S*-transferase; GFP, green fluorescent protein.

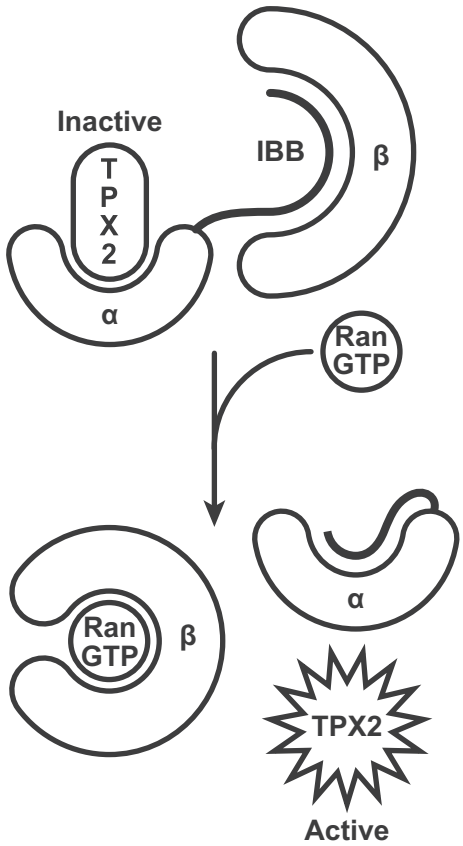

FIGURE 1. **Schematic illustration of how TPX2 is activated by RanGTP in the vicinity of the chromosomes.** In the bulk of the cytoplasm, where the RanGTP concentration is low, importin-α binds to importin-β via its IBB domain freeing it to bind to TPX2 thereby inactivating its role in mitotic spindle assembly (1–3). However near the chromosomes, where the RanGTP concentration is elevated (11), RanGTP binds to importin-β leading to the release of TPX2 from importin-α, after which TPX2 is active in mitotic spindle assembly.

series of tandem "ARM" repeats, each of which is based on a motif containing three α-helices (20). NLSs bind to the inner concave surface of importin-α through interactions with a series of strategically located Trp, Asn, and acidic residues (reviewed in Refs. 5, 6, 12). In addition to the ARM repeats, importin-α also has a region of ~70 residues at its N terminus that binds to importin-β. This importin-β-binding domain (IBB) also has an auto-inhibitory role such that, when it is not bound to importin-β (most commonly when RanGTP is bound to importin-β), it can bind to the inner surface of importin-α and reduce its affinity for bound NLSs (13). Dissociation of the NLS is then completed using additional factors, such as Cse1/CAS (5, 6).

NLSs are either monopartite, consisting of a single cluster of positively charged residues, or bipartite, based on two positively charged clusters separated by ~10 residues, although in some cases somewhat longer linkers have been observed (21). The residues binding to the major site are designated P1-P5 and those binding to the minor site as P′1-P′4 (Fig. 3*D*). Monopartite NLSs bind primarily to a site, generally referred to as the "major NLS-binding site," located on ARM repeats 2–4, whereas bipartite NLSs bind to both this site and a second "minor" site, located on ARM repeats 7 and 8 (20, 22, 23). However, monopartite NLSs also bind to the minor site, but with lower affinity (20, 22, 23). Extensive mutagenesis and biophysical studies (23–30; reviewed in Ref. 12) have established the contributions made to the interaction by residues located at the different positions within the NLSs. It is crucial to have Lys in position P2 (25) to enable salt-bridge formation with Asp-192 and even mutation to Arg shows greatly reduced nuclear accumulation (29). Position P4, conversely, makes a smaller contribution to the binding energy (25) and shows much greater variability between different NLSs. Positions P3 and P5 are usually Lys or Arg and make intermediate contributions to the binding energy (25). The binding of Lys and Arg in positions P′1 and P′2 is thought to be the primary interaction at the minor NLS-binding site, with reduced contributions being made by the residues at positions P′3 and P′4 (24, 25, 27).

Although TPX2 binds to importin-α, it does not contain a classical NLS and instead employs a sequence including Lys-284 and Arg-285 (31). Mutation of these residues prevents importin-α from inhibiting TPX2-mediated microtubule assembly, as does mutation of the two sites on importin-α that are responsible for binding NLSs (7, 31). It is to some extent paradoxical that importin-α can inhibit TPX2 so effectively in mitotic cells because a great number of normally nuclear proteins that contain classical NLSs will become accessible following nuclear envelope breakdown. Here we characterize the TPX2:importin-α interaction more fully, using a combination of structural and biochemical approaches, to establish how TPX2 binds to importin-α. We find two regions of TPX2 that interact with importin-α, one of which contains primarily residues 284–287 identified earlier (31), and a second region that contains primarily residues 327–330. Of these regions, residues 284–287 bind more strongly and are the primary determinant of the interaction. However, these residues unexpectedly bind to the minor NLS-binding site on importin-α rather than the major site. Instead, residues 327–330 bind to the major NLS-binding site even though they do not correspond closely to the consensus binding sequence seen with classical monopartite NLSs. The predominant role of the minor NLS-binding site in the TPX2:importin-α interaction may account to some extent for ability of importin-α to bind TPX2 in the presence of many other proteins that contain a monopartite NLS and opens the possibility of generating small molecule inhibitors that may selectively inhibit this interaction.

EXPERIMENTAL PROCEDURES

Expression and Purification of the TPX2-NLS:ΔIBB-Importin-α Complex—A fragment ($TPX2^{270-350}$) corresponding to residues 270–350 of *Xenopus* TPX2 (GI: 46249461) was cloned into pGEX-TEV (14) and expressed as GST fusions in *Escherichia coli* BL21(DE3) CodonPlus RIL cells at 20 °C overnight. Untagged mouse importin-α lacking the IBB domain (residues 70–529, ΔIBB-importin-α) was expressed as described (15). All subsequent steps were performed at 4 °C. After harvesting, the two sets of cells were lysed in 50 mM Tris-HCl (pH 7.4), 200 mM NaCl, 2 mM DTT by high-pressure cavitation (15k psi). Clarified cell lysates were mixed and incubated with glutathione-Sepharose for 1 h. After washing the beads extensively, the complex was released from the resin by overnight

digestion with His-TEV protease (S219V mutant; Ref. 32). The complex was further purified by gel filtration on a Superdex 75 26/60 column in 20 mM Tris-HCl (pH 7.4), 100 mM NaCl, and 2 mM DTT and concentrated to 20 mg/ml.

Cloning, Expression, and Purification of Proteins for Biochemical Assays—GST fusions containing the SV40 NLS or nucleoplasmin NLS were expressed and purified as described (33). GST-TPX2$^{270-289}$ and GST-TPX2$^{290-350}$ were expressed from pGEX-TEV, whereas TPX2$^{276-291}$-GFP and TPX2$^{276-351}$-GFP were expressed from pET28a. *Xenopus* and mouse ΔIBB-importin-α constructs were expressed from pET30a as His/S-fusions. The cDNAs employed were for mouse: importin-α1, GI: 13879578; importin-α3, GI: 20073210; mouse-α4, GI: 2007072; importin-α6, GI: 13436001; and importin-α2; GI: 6754474; for *Xenopus*: importin-α1a, GI: 67678145; importin-α2, GI: 27696874; and importin-α5.2, GI: 48734621. Mutations in *Xenopus* ΔIBB-importin-α1a and mouse ΔIBB-importin-α2 were introduced by site-directed mutagenesis to create the following mutant constructs: mouse ΔIBB-importin-αED (D192K/E396R), mouse ΔIBB-importin-αE (E396R), mouse ΔIBB-importin-αD (D192K), *Xenopus* ΔIBB-importin-αED (D189K, E389R), *Xenopus* ΔIBB-importin-αED (E389R), and *Xenopus* ΔIBB-importin-αD (D189K). The resultant cDNAs were then cloned into pET30a using BamHI and EcoRI sites.

All constructs were verified by sequencing. Recombinant proteins were expressed in BL21(DE3) CodonPlus RIL cells at 20 °C overnight. His/S tagged importin-α constructs, TPX2$^{276-291}$-GFP, and TPX2$^{276-351}$-GFP were purified over Ni-NTA (Qiagen) following the manufacturer's protocols. Proteins were further purified by gel filtration over Superdex 75 in 20 mM Tris-HCl (pH 7.4), 100 mM NaCl, and 5 mM 2-mercaptoethanol. GST fusion proteins for pull-down experiments were purified over glutathione-Sepharose 4B (Amersham Biosciences) as described by the manufacturer.

In Vitro Pull-down Assays—For standard pull-down assays, clarified bacterial cell lysates expressing the respective GST fusions were bound to glutathione-Sepharose and incubated with cell lysates expressing the various importin-α constructs. For competition pull-down experiments, GST-NLS fusion proteins (4.5 μg) were bound to 10 μl of glutathione Sepharose and incubated with ΔIBB-importin-α (10 μg) ± 30 μM of the indicated TPX2-GFP constructs in 100 μl of binding buffer (PBS, 0.1% Tween-20 and 2 mM DTT) for 1 h at 4 °C. Beads were washed 3× in 500 μl of binding buffer, and bound proteins were subsequently eluted with SDS-sample buffer. Bound and unbound fractions were analyzed on SDS-PAGE gels stained with Coomassie Blue.

Crystallography—Crystals of the TPX2:importin-α complex were obtained by hanging drop vapor diffusion in which 2-μl drops of protein solution were mixed with 2 μl drops of well buffer containing 100 mM Tris-HCl (pH 7.0), 1.1–1.2 M ammonium sulfate and 10 mM DTT and equilibrated in Linbro plates at 18 °C. Diffraction data were collected from single crystals soaked briefly in crystallization buffer supplemented with 20% glycerol and flash frozen at 100 K in a nitrogen stream. A native data set was obtained using beamline ID29 at the European Synchrotron Research facility (ESRF), Grenoble, France (Table 1). The crystals had $P2_12_12_1$ orthorhombic symmetry with and were isomorphous to the crystals formed by the complex between importin-α: and the nucleoplasmin NLS (Ref. 23; PDB accession code 1EYJ). The importin-α chain was positioned by rigid body refinement and then subjected to iterative cycles of refinement and rebuilding using PHENIX (34) with TLS (35) and COOT (36), after which there was clear difference density located in both NLS-binding pockets and many side chains of the bound peptide could be identified unequivocally. TPX2 residues 283–288 were built into the density located at the minor site whereas residues 322–331 were built into the major site. There was very clear side-chain density for the residue in position P1 in the major NLS-binding site, which confirmed that the principal TPX2 NLS was not bound in this position (because the corresponding residue would be Gly). A final model was obtained after further cycles of refinement and rebuilding and the addition of five sulfate ions and 227 waters. Table 1 gives the crystallographic statistics.

The atomic coordinates and structure factors (code 3KND) have been deposited in the Protein Data Bank, Research Collaboratory for Structural Bioinformatics, Rutgers University, New Brunswick, NJ.

RESULTS

Residues 270–289 of TPX2 Bind to a Range of Importin-α Isoforms—Nuclear localization sequences usually bind to a broad range of different importin-α isoforms from different species (12, 37, 38). Both the SV40 monopartite NLS and nucleoplasmin bipartite NLS, for example, bind to yeast and mammalian importin-α. However, the *Xenopus* TPX2 NLS that binds to importin-α involves a sequence around two basic residues at positions 284 and 285 that does not fit the classical NLS consensus (31). Although the precise boundaries of the TPX2 NLS had not been established in earlier work, we found that a fragment containing residues 270–289 (TPX2$^{270-289}$) was able to bind a range of vertebrate importin-α constructs from which the autoinhibitory IBB domain had been deleted (Fig. 2). The ΔIBB-importin-α constructs mimic the importin-α:β complex that binds NLSs *in vivo* (12). Thus, GST-TPX2$^{270-289}$was able to bind specifically to ΔIBB constructs of *Xenopus* importin-α1a, -α2, and -α5.2 and also mouse importin-α1, -α2, -α4, and -α6, from crude bacterial lysates, whereas negligible binding was seen to GST alone. This result was consistent with the TPX2 NLS having the broad binding specificity seen with classical NLSs.

Crystal Structure of a TPX2:Importin-α Complex—Attempts to crystallize ΔIBB-importin-α complexed with TPX2$^{276-289}$ only resulted in very small crystals that were not suitable for data collection. Therefore, we screened complexes of ΔIBB-importin-α bound to a range of longer TPX2 fragments and found that the complex formed with TPX2 residues 270–350 yielded crystals with $P2_12_12_1$ orthorhombic symmetry that diffracted to 2.2 Å resolution using synchrotron radiation (Table 1). The crystals were isomorphous with those obtained previously for the importin-α:nucleoplasmin-NLS complex (Ref. 23; PDB accession number 1EYJ) and rigid body refinement enabled the importin-α chain to be modeled using the structure determined previously. After initial refinement and rebuilding, there was clear density located over both the minor and major NLS

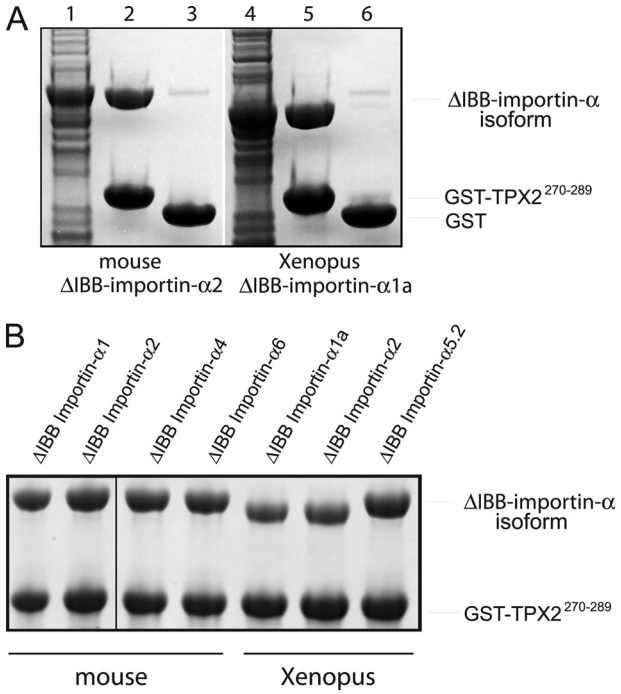

FIGURE 2. **The TPX2$^{270-289}$ NLS binds to a range of *Xenopus* and mouse importin-α constructs.** *A*, *lanes 1* and *4* are crude bacterial lysate expressing the importin-α isoform; *lanes 2* and *5* are the pull-down using GST-TPX2$^{270-289}$; and *lanes 3* and *6* are the pull-down using GST alone. GST-TPX2$^{270-289}$ was able to bind mouse ΔIBB-importin-α2 and *Xenopus* ΔIBB-importin-α1a specifically from crude bacterial lysates, whereas virtually no binding was seen to GST alone. *B*, GST-TPX2$^{270-289}$ binds to a range of ΔIBB importin-α isoforms derived from either mouse or *Xenopus*.

TABLE 1
Crystallography data

Crystals	
Symmetry	$P2_12_12_1$
a, b, c (Å)	78.53, 89.32, 99.27
Data collection	
Wavelength (Å)	0.9814
Resolution range (Å)[a]	27.85–2.2 (2.32–2.2)
Total observations[a]	248850 (35541)
Unique observations[a]	36138 (5187)
Completeness (%)[a]	99.9 (100)
Multiplicity	6.9 (6.9)
R_{pim} (%)[a]	4.6 (39.9)
Mean I/σ(I)[a]	11.7 (2.2)
Refinement	
R_{cryst}/R_{free} (%)	18.8/21.2
Bond length rmsd (Å)	0.003
Bond angle rmsd (°)	0.75
MolProbity score/percentile	1.24/100
Ramachandran plot (%)	
Favored	99.1
Allowed	0.9
Forbidden	0
PDB accession number:	3KND

[a] Parentheses refer to final resolution shell.

binding pockets (Fig. 3*A*). Although this density was not continuous, the sequence of fragments corresponding to residues 283–288 and 322–331 of TPX2 could be built easily into the difference density and, after adding five sulfates and 227 waters, resulted in a final structural model with an *R*-factor of 18.3% (R_{free} 21.2%), excellent geometry (Table 1) and a MolProbity (39) score of 1.24 (100th percentile). No reliable electron density was seen for the remaining residues in the TPX2 fragment.

The structural model (Fig. 3) showed that the primary TPX2 NLS, comprising residues 284–287 (KRKH, Ref. 31) was bound to the "minor" NLS-binding site on importin-α (located primarily in ARM repeats 7 and 8), whereas TPX2 residues 327–330 (KMIK) were bound to the "major" NLS-binding site (located primarily in ARM repeats 2–4). Density from several residues outside this range was also visible, but was weaker, consistent with these two four-residue regions forming the principal interfaces between the TPX2 peptide and importin-α. Fig. 3 shows the details of the interaction at each site, together with a comparison with the interactions seen with the nucleoplasmin NLS (23). The TPX2 residues at the minor site formed an extensive network of interactions with importin-α. Lysine 284 in position P′1 formed H-bonds with Thr-328, Ser-361 and the main-chain carbonyl of Val-321; the side chain of Arg-285, in position P′2, was sandwiched between the indole rings of Trp-357 and Trp-399 and formed a salt-bridge to Glu-396; Lys-286, in position P′3, formed H-bonds with Thr-322 and Asn-283 and also to the main chain of Gly-281; and His-287, in position P′4, formed a salt bridge with Glu-354 and extensive hydrophobic/π interactions with Trp-357. Additional H-bonds were formed to the NLSs main chain by Trp-357and Gln-361. In the major NLS-binding site, Lys-327, in position P2, formed a salt bridge with Asp-192, together with H-bonds to Thr-155 and the main-chain carbonyl of Gly-150; Met-328, in position P3, was sandwiched between the indole rings of Trp-184 and Trp-223 in a conformation similar to that seen with Lys or Arg in classic NLSs; and Lys-330, in position P5, was sandwiched between the indole rings of Trp-142 and Trp-184. There were also a series of H-bonds formed between the main-chain carbonyls of the NLS and Asn-146, Asn-188, and Asn-235. Ser-324 also formed H-bonds with Arg-238 and Tyr-277.

Importin-α Variants Confirm that TPX2$^{283-287}$ Binds to the Minor NLS-binding Site—Previous work showed that specific point mutations in importin-α can inhibit binding in either the major or minor NLS-binding site selectively (7, 28, 31). Thus, in yeast (28), the D203K variant inhibits binding to the major site whereas E402R inhibits binding to the minor site (the equivalent mutants in mouse and *Xenopus* importin-α are D192K/E396R and D189K/E389R, respectively). We therefore constructed the corresponding mouse and *Xenopus* ΔIBB importin-α variants that contained mutations in the major (ΔIBB-importin-αD) and minor (ΔIBB-importin-αE) NLS binding site either individually, or in both sites (ΔIBB-importin-αED) simultaneously. These variants were then tested for their ability to bind to the TPX2$^{270-289}$and TPX2$^{270-350}$ NLS constructs and also to the monopartite SV40 NLS and bipartite nucleoplasmin NLS as controls.

GST-NLS fusions were coupled to glutathione Sepharose and used for pull-down experiments with the ΔIBB-importin-α variants. None of the ΔIBB-importin-α variants bound to GST alone (data not shown). Both *Xenopus* and mouse ΔIBB-importin-α bound the TPX2$^{270-289}$and TPX2$^{270-350}$ NLS fragments in a similar manner (Fig. 4, *A* and *B*). Although the TPX2, SV40, and nucleoplasmin NLSs all bound wild-type *Xenopus* and mouse ΔIBB-importin-α, no binding could be detected for any NLS to the ΔIBB importin-αED mutant. Consistent with previous work (28, 37), the nucleoplasmin and the SV40 NLS still

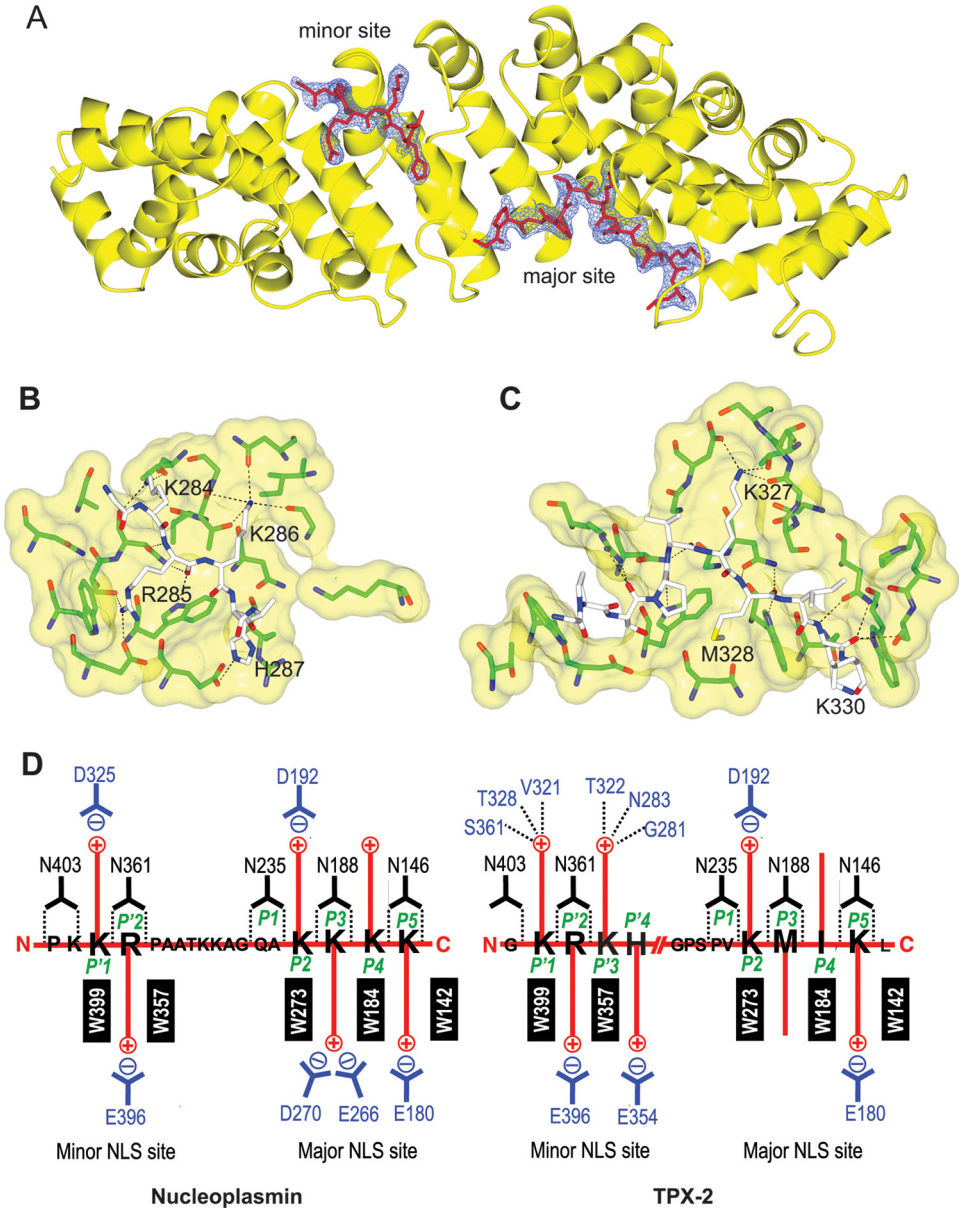

FIGURE 3. **Crystal structure of the TPX2:ΔIBB-importin-α complex.** *A*, electron density (*blue*) for the TPX2 NLS peptide (*red*) superimposed on the importin-α structure (*yellow*); *B*, interaction interface between TPX2 residues 283–288 and the minor NLS-binding site on importin-α; *C*, interaction interface between TPX2 residues 322–331 and the major NLS-binding site on importin-α; *D*, schematic illustration of the interactions of importin-α with nucleoplasmin and TPX2, respectively.

bound the ΔIBB-importin-αE variants, but did not bind the D variant. In contrast, both TPX2 NLS fragments interacted efficiently with the D variant but not with the E variant, confirming that $TPX2^{284-287}$ binds primarily to the minor NLS-binding site of importin-α.

$TPX2^{284-287}$ Represents the Principal Importin-α-binding Site—Because the crystal structure of the TPX2:importin-α complex identified two TPX2 regions that bind to importin-α, we investigated the relative contribution made by each site. GST fusions containing either $TPX2^{270-289}$ or $TPX2^{290-350}$ were bound to glutathione-Sepharose and probed with ΔIBB-importin-α (Fig. 5). A control fragment containing both TPX2-binding segments ($TPX2^{270-350}$) and also $TPX2^{270-289}$ were able to pull-down ΔIBB-importin-α from bacterial lysates. In contrast, the $TPX2^{290-350}$ fragment that contained only the second TPX2 importin-α-binding region was not able to pull down importin-α, indicating that removing $TPX2^{284-287}$ reduced the binding of TPX2 to importin-α dramatically. Therefore, the binding site on TPX2 containing residues 284–287 is crucial for the interaction with importin-α.

Competition for Importin-α—We used a pull-down assay to evaluate the extent to which TPX2 and other NLSs competed for binding to ΔIBB-importin-α. Immobilized GST-SV40 NLS or GST-nucleoplasmin NLS was incubated simultaneously with *Xenopus* ΔIBB-importin-α and TPX2 NLS fragments consisting of either both binding sites ($TPX2^{284-287}$ and $TPX2^{327-330}$) or $TPX2^{284-287}$ alone fused to the N terminus of GFP ($TPX2^{276-291}$-GFP or $TPX2^{276-351}$-GFP, respectively). In the presence of $TPX2^{284-287}$, only a small amount of ΔIBB-importin-α was displaced from the SV40 NLS, as evidenced by the decrease in ΔIBB-importin-α in the fraction remaining bound to the beads after centrifugation, and a corresponding increase in the unbound fraction that remained in solution (Fig. 6). However, despite its being somewhat degraded by proteolysis, the $TPX2^{276-351}$ fragment containing both binding sites displaced most of the ΔIBB-importin-α from SV40 NLS, so that only a small amount of ΔIBB-importin-α remained bound while the concentration of ΔIBB-importin-α in the unbound fraction increased markedly. The $TPX2^{276-291}$ only displaced a small amount of ΔIBB-importin-α bound to the nucleoplasmin-NLS, but considerably more ΔIBB-importin-α was displaced, as evidenced by the increase in ΔIBB-importin-α in the unbound fraction when the $TPX2^{276-351}$ fragment that contained both sites was employed. The $TPX2^{276-351}$ fragment was very labile to proteolysis, even in the presence of a mixture of inhibitors, probably because it was mainly unstructured in solution. However, even in its degraded form it was able to compete for binding to ΔIBB-importin-α to a considerable extent. The nucleoplasmin NLS has a higher affinity for ΔIBB-importin-α than the SV40 NLS (12, 15, 24, 25), and so it was to be expected that it would be more difficult for TPX2 to displace it.

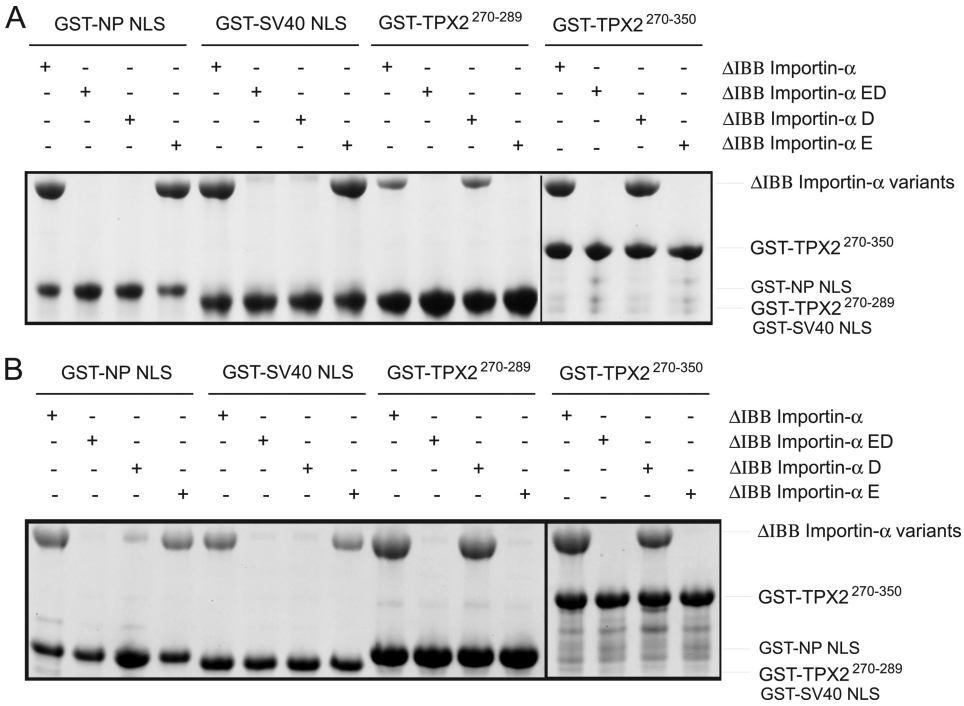

FIGURE 4. **Nonclassical TPX2 NLS binds to the minor binding site of ΔIBB importin-α.** Pull-down assays with ΔIBB importin-α variants from mouse (*A*) and *Xenopus* (*B*). Clarified bacterial cell lysates expressing the indicated GST fusion proteins were immobilized on glutathione-Sepharose and incubated with cell lysates containing the respective importin-α variants. Bound proteins were eluted with 2× SDS sample buffer and analyzed by SDS-PAGE. The ΔIBB importin-αD and ΔIBB importin-αE are variants in which binding to the major and minor binding sites, respectively, is inhibited, whereas the ΔIBB importin-αED variant harbors mutations in both sites.

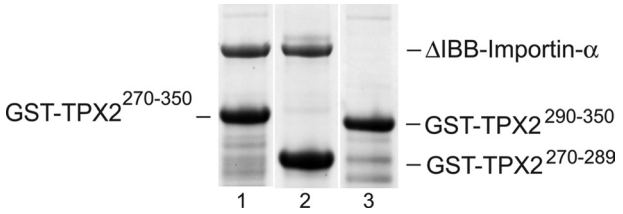

FIGURE 5. **TPX2 284–287 is the stronger binding site for ΔIBB importin-α.** Pull-down assays were performed with crude bacterial cell lysates expressing the indicated GST-TPX2 NLS fragments to assess their ability to co-precipitate ΔIBB importin-α. Whereas TPX2 fragments containing residues 284–287 (GST-TPX2 270–350, *lane 1*, and GST-TPX2 270–289, *lane 2*) were able to pull-down ΔIBB-importin-α, the fragment containing only residues 322–331 (GST-TPX2 290–350, *lane 3*) was not, consistent with residues 284–287 representing the major importin-α-binding site on TPX2.

DISCUSSION

Both the crystal structure of the TPX2:importin-α complex and the binding studies with importin variants support the primary TPX2 NLS (^{284}KRKH^{287}) binding to the minor NLS-binding site on importin-α. Moreover, the binding studies indicate that this interaction makes a greater contribution to the binding than the interaction seen between TPX2 ^{327}KMIK^{330} and the major NLS binding site. This is the converse to the usual observation with bipartite NLSs, where the interaction with the major NLS-binding site makes the greater contribution.

Neither interaction observed with the two TPX2 regions that bound to importin-α was typical of that seen with other NLSs bound to importin-α. The crystal structures of NLSs derived from nucleoplasmin (23), neuroblastoma protein (27), phosphoprotein N1N2 (27), and CBP80 (40) bound to importin-α have been obtained. All of these classical bipartite NLSs had a cluster of positively-charged residues (KKKK, KKLR, KKSK, and KRRK, respectively) bound to positions P2-P5 of the "major" NLS-binding site. In contrast, TPX2 bound KMIK at the major site and so retained a positively charged side chain only at positions P2 and P5. However, although this sequence does not fit the consensus binding motif for the major NLS binding site, many of the interactions observed with both bipartite and monopartite NLSs with the major binding site on importin-α were preserved, especially those that extensive mutagenesis studies (24, 25) have shown to be more important for binding. Thus, Lys-327 in position P2, which has been shown to make the most important contribution to the binding energy (25), forms a salt-bridge with Asp-192 and there is a series of H-bonds between the TPX2 main chain carbonyls and Asn-145, Asn-188, and Asn-235. Moreover, Lys-330 in position P5, which makes the next most-important contribution, is also conserved. In position P3, Met-328 is sandwiched between Trp-184 and Trp-231 analogous to the way in which a Lys or Arg chain is usually positioned (23, 27). Although this interaction would lack the cation-π interaction (41) seen conventionally, the contribution made from the hydrophobic interaction would be still substantial.

The interaction between the TPX2 NLS and the "minor" NLS-binding site on importin-α is much more extensive than observed with typical classical NLSs. Although the binding of Lys-284 and Arg-285 in positions P′1 and P′2, respectively, is similar to that observed with bipartite classical NLSs, Lys-286 and His-287 also make extensive interactions with importin-α. Thus, in addition to the contribution due to burying hydrophobic surfaces, Lys-286, in position P′3, forms H-bonded networks with Gly-281, Asn-283, and Thr-322, whereas His-287, in position P′4, forms a putative salt bridge with Glu-354 as well as an extensive cation-π interaction (41) with Trp-357. Although the 40 residues separating the two importin-α binding clusters on TPX2 is much greater than the 10–12 more commonly observed for bipartite NLSs, there are examples of longer linkers that can be accommodated provided they are sufficiently flexible (21).

Recent work (37, 38) has used a universal GFP expression system to screen random peptide libraries to identify six classes of NLS that bind to importin-α. Three of these classes corresponded to the classical monopartite (classes 1 and 2) and bipartite (class 6) NLSs, whereas class 5 was plant-specific. However, two classes were identified that appeared to bind

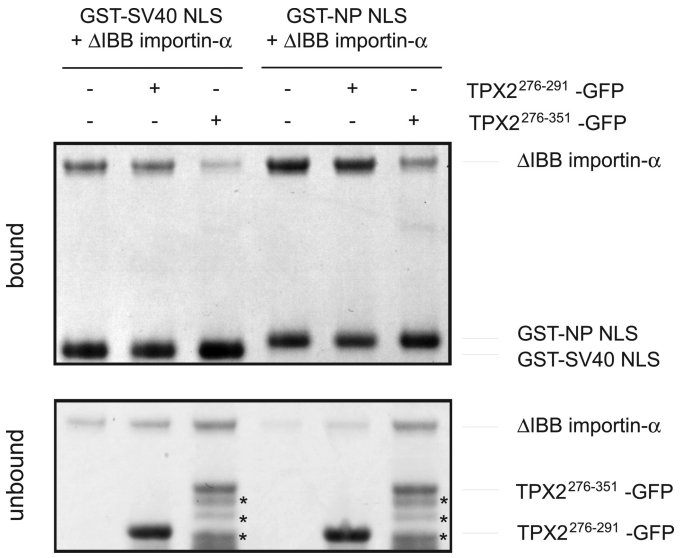

FIGURE 6. **Pull-down competition assay.** Beads containing 4.5 μg of GST-SV40 NLS (*lanes 1–3*) or 4.5 μg of GST-nucleoplasmin NLS (*lanes 4–6*) were incubated with 10 μg of ΔIBB importin-α ± 30 μM of the indicated TPX2 NLS-GFP fragments. Following incubation, the beads were separated and washed by centrifugation. The *bound* lane shows the material remaining on the beads, whereas the *unbound* is the material remaining in solution. Although it has been proteolyzed to a considerable extent $TPX2^{276-351}$-GFP can compete with both the SV40, and the nucleoplasmin NLS for binding to ΔIBB-importin-α, as evidenced by the displacement of ΔIBB-importin-α from the GST-NLS into the unbound fraction, whereas $TPX2^{276-291}$-GFP competes less effectively, so that more ΔIBB-importin-α remains bound. *Asterisks* represent impurities or proteolytic fragments.

preferentially to the minor NLS-binding site on importin-α. Class 3 had the consensus sequence KR*X*[WFYH]*XX*AF, whereas class 4 had the consensus [RP]*XX*KRR[KR][-DE], where *X* represents any residue, square brackets indicate any of the residues that can be found at that position, and "-" indicates residues that are not found at the position. Neither monopartite (classes 1 and 2) consensus sequence corresponds to the TPX2 sequence ^{327}KMIK^{330} found at the major site, nor does either minor site NLS consensus sequence (classes 3 and 4) match the $TPX2^{284-287}$ KRKH sequence. However, His-287 could correspond to the large hydrophobic residue often found at position 4 in the class 3 consensus and which has been found to be effective for nuclear protein import in yeast (38), although these experiments did not distinguish between major and minor site binding. Interestingly, in class 3, sequences with a consensus RK*X*[WFY]*XX*AF (in which the K and R in positions 1 and 2 were exchanged) or in which the R in position 2 was mutated to any other residue showed greatly reduced binding to importin-α, consistent with the crucial roles of these residues in the TPX2 sequence.

Although the $TPX2^{284-287}$ NLS is based on four consecutive positively charged residues (KRKH), it clearly does not bind strongly to the major site on importin-α. In classical NLSs, a Lys or Arg in position P5 forms a prominent cation-π interaction with importin-α Trps 142 and 184 that makes a considerable contribution to the binding energy that is second only to that made by the Lys in position P2 (25). Although His-287 is also positively charged, the charge is located closer to the NLS main chain than with Lys or Arg and is more distant from Gln-181 with which these residues form a putative H-bond. This, combined with the rigidity of the imidazole ring, probably result in His-287 making a considerably reduced contribution to the binding energy of the $TPX2^{284-287}$ NLS to the major NLS-binding site on importin-α. An analogous sequence may function in the C-terminal kinesin XCTK2 that is important for spindle assembly. XCTK2 is inhibited by importin-α and here the sequence ^{19}KRKY^{22} is crucial for the interaction (42). Although it has not been established whether XCTK2 binds primarily to the minor NLS-binding site on importin-α, it is likely that here Tyr-22 could function similarly to His-287 in TPX2.

The atypical way in which TPX2 binds to importin-α, with the more important interaction taking place at the minor NLS-binding site, would reduce the competition for binding from other proteins containing NLSs, especially the more common monopartite variety exemplified by SV40 (12) that binds primarily to the major NLS-binding site on importin-α. In the bulk of the cytoplasm, away from the chromosomes, the RanGTP concentration is too low to dissociate the importin-α:β complex which is then able to bind TPX2 and inactivate it (7–10). It is in this region that competition from other NLSs could potentially cause a problem because if importin-α were to be saturated with other NLSs this could inhibit its binding to TPX2 and inactivating it. This could in turn lead to aberrant spindle formation away from the chromosomes. By contrast, near the chromosomes, where the RanGTP concentration is elevated (11), RanGTP binds to importin-β leading to the release of TPX2 locally to participate in spindle assembly. However, because monopartite NLSs still bind to the minor site on importin-α with reduced affinity (22, 23), adding a large excess, especially of a polydentate conjugate of NLSs with BSA, would still have the potential to displace TPX2 from importin-α as observed by Schatz *et al.* (31). Moreover, although nucleoplasmin binds more strongly to importin-α than the SV40 NLS (12, 15, 23–27), during mitosis this protein is heavily phosphorylated and also binds strongly to histones, both of which may impede its binding to importin-α. Because of the unusual way in which TPX2 binds to importin-α, the detailed knowledge of the interaction interface provided by the present crystal structure may facilitate the construction of specific small molecule inhibitors that may interfere with the mitotic TPX2:importin-α interaction while not altering the interphase nuclear protein import function, at least with respect to monopartite NLS-containing cargoes.

Acknowledgments—We thank our colleagues in Cambridge, especially Neil Marshall, Andrew Ellisdon, Florian Gruessing, Rhian Tolvey, and Christoph Brockmann, for many helpful comments, criticisms, and suggestions; Danguole Ciziene for technical assistance; and Jo Westmoreland for illustrations. We thank Mark Allen and Gordon Leonard for data collection at ESRF.

REFERENCES

1. Gruss, O. J., and Vernos, I. (2004) *J. Cell Biol.* **166,** 949–955
2. Bastiaens, P., Caudron, M., Niethammer, P., and Karsenti, E. (2006) *Trends Cell Biol.* **16,** 125–134
3. Clarke, P. R., and Zhang, C. (2008) *Nat. Rev. Mol. Cell Biol.* **9,** 464–477
4. Walczak, C. E., and Heald, R. (2008) *Int Rev Cytol.* **265,** 111–158
5. Cook, A., Bono, F., Jinek, M., and Conti, E. (2007) *Annu. Rev. Biochem.* **76,**

647–671
6. Stewart, M. (2007) *Nat. Rev. Mol. Cell Biol.* **8,** 195–208
7. Gruss, O. J., Carazo-Salas, R. E., Schatz, C. A., Guarguaglini, G., Kast. J., Wilm, M., Le Bot, N., Vernos, I., Karsenti, E., and Mattaj, I. W. (2001) *Cell* **104,** 83–93
8. Gruss, O. J., Wittmann, M., Yokoyama, H., Pepperkok, R., Kufer, T., Silljé, H., Karsenti, E., Mattaj, I. W., and Vernos, I. (2002) *Nat. Cell Biol.* **4,** 871–879
9. Tsai, M. Y., Wiese, C., Cao, K., Martin, O., Donovan, P., Ruderman, J., Prigent, C., and Zheng, Y. (2003) *Nat. Cell Biol.* **5,** 242–248
10. Groen, A. C., Maresca, T. J., Gatlin, J. C., Salmon, E. D., and Mitchison, T. J. (2009) *Mol. Biol. Cell* **20,** 2766–2773
11. Kalab, P., and Heald, R. (2008) *J. Cell Sci.* **121,** 1577–1586
12. Lange, A., Mills, R. E., Lange, C. J., Stewart, M., Devine, S. E., and Corbett, A. H. (2007) *J. Biol. Chem.* **282,** 5101–5105
13. Kobe, B. (1999) *Nat. Struct. Biol.* **6,** 388–397
14. Matsuura, Y., and Stewart, M. (2004) *Nature* **432,** 872–877
15. Matsuura, Y., and Stewart, M. (2005) *EMBO J.* **24,** 3681–3689
16. Bibby, R. A., Tang, C., Faisal, A., Drosopoulos, K., Lubbe, S., Houlston, R., Bayliss, R., and Linardopoulos, S. (2009) *J. Biol. Chem.* **284,** 33177–33184
17. Brunet, S., Sardon, T., Zimmerman, T., Wittmann, T., Pepperkok, R., Karsenti, E., and Vernos, I. (2004) *Mol. Biol. Cell* **15,** 5318–5328
18. Eckerdt, F., Eyers, P. A., Lewellyn, A. L., Prigent, C., and Maller, J. L. (2008) *Curr. Biol.* **18,** 519–525
19. Tulu, U. S., Fagerstrom, C., Ferenz, N. P., and Wadsworth, P. (2006) *Curr. Biol.* **16,** 536–541
20. Conti, E., Uy, M., Leighton, L., Blobel, G., and Kuriyan, J. (1998) *Cell* **94,** 193–204
21. Lange, A., McLane, L. M., Mills, R. E., Devine, S. E., and Corbett, A. H. (2010) *Traffic* **11,** 311–323
22. Conti, E., and Kuriyan, J. (2000) *Structure* **8,** 329–338
23. Fontes, M. R., Teh, T., and Kobe, B. (2000) *J. Mol. Biol.* **297,** 1183–1194
24. Catimel, B., Teh, T., Fontes, M. R., Jennings, I. G., Jans, D. A., Howlett, G. J., Nice, E. C., and Kobe, B. (2001) *J. Biol. Chem.* **276,** 34189–34198
25. Hodel, M. R., Corbett, A. H., and Hodel, A. E. (2001) *J. Biol. Chem.* **276,** 1317–1325
26. Hodel, A. E., Harreman, M. T., Pulliam, K. F., Harben, M. E., Holmes, J. S., Hodel, M. R., Berland, K. M., and Corbett, A. H. (2006) *J. Biol. Chem.* **281,** 23545–23556
27. Fontes, M. R., Teh, T., Jans, D., Brinkworth, R. I., and Kobe, B. (2003) *J. Biol. Chem.* **278,** 27981–27987
28. Leung, S. W., Harremann, M. T., Hodel, M. R., Hodel, A. E., and Corbett, A. H. (2003) *J. Biol. Chem.* **278,** 41947–41953
29. Harreman, M. T., Kline, T. M., Milford, H. G., Harben, M. B., Hodel, A. E., and Corbett, A. H. (2004) *J. Biol. Chem.* **279,** 20613–20621
30. Colledge, W. H., Richardson, W. D., Edge, M. D., and Smith. A. E. (1986) *Mol. Cell. Biol.* **6,** 4136–4139
31. Schatz, C. A., Santarella, R., Hoenger, A., Karsenti, E., Mattaj, I. W., Gruss, O. J., and Carazo-Salas, R. E. (2003) *EMBO J.* **22,** 2060–2070
32. Kapust, R. B., Tözsér, J., Fox, J. D., Anderson, D. E., Cherry, S., Copeland, T. D., and Waugh, D. S. (2001) *Protein Eng.* **14,** 993–1000
33. Matsuura, Y., Lange, A., Harriman, M. T., Corbett, A. H., and Stewart, M. (2003) *EMBO J.* **22,** 5358–5369
34. Adams, P. D., Grosse-Kunstleve, R. W., Hung, L. W., Ioerger, T. R., McCoy, A. J., Moriarty, N. W., Read, R. J., Sacchettini, J. C., Sauter, N. K., and Terwilliger, T. C. (2002) *Acta Crystallogr.* **D58,** 1948–1954
35. Painter, J., and Merritt, E. A. (2006) *J. Appl. Crystallogr.* **39,** 109–111
36. Emsley, P., and Cowtan, K. (2004) *Acta Cryst.* **D60,** 2126–2132
37. Kosugi, S., Hasebe, M., Matsumura, N., Takashima, H., Miyamoto-Sato, E., Tomita, M., and Yanagawa, H. (2009) *J. Biol. Chem.* **284,** 478–485
38. Kosugi, S., Hasebe, M., Tomita, M., and Yanagawa, H. (2009) *Proc. Natl. Acad. Sci., U.S.A.* **106,** 10171–10176
39. Davis, I. W., Leaver-Fay, A., Chen, V. B., Block, J. N., Kapral, G. J., Wang, X., Murray, L. W., Arendall, W. B., 3rd, Snoeyink, J., Richardson, J. S., and Richardson, D. C. (2007) *Nucleic Acids Res.* **35,** W375–W383
40. Dias, S. M., Wilson, K. F., Rojas, K. S., Ambrosio, A. L., and Cerione, R. A. (2009) *Nat. Struct. Mol. Biol.* **16,** 930–937
41. Dougherty, D. A. (1996) *Science* **271,** 163–168
42. Ems-McClung, S. C., Zheng, Y., and Walczak, C. E. (2004) *Mol. Biol. Cell* **15,** 46–57